

Montana Bureau of Mines and Geology EDMAP 4

**GEOLOGIC MAP OF PARTS OF THE CARLTON LAKE, DICK CREEK AND
WEST FORK BUTTE 7.5' QUADRANGLES, WESTERN MONTANA**

by

Connie Brown, Colleen Fitzpatrick, and Julia A. Baldwin
The University of Montana

2009

This report was prepared by geology students under the direction of his advisor as a product of the EDMAP Component of the U.S. Geological Survey National Cooperative Geologic Mapping Program, Contract Number 06HQAG0079. It has not been reviewed by the Montana Bureau of Mines and Geology and does not necessarily conform to the usual style and standards for Bureau publications.

Introduction

The field area for this project is about 18 km west of Lolo, Montana (Figure 1). The western half of the field area (West Fork Butte and Dick Creek 7.5' quadrangles) contains the Skookum Butte stock, a satellite pluton of the Idaho-Bitterroot batholith (IBB). The eastern part (Carlton Lake quadrangle 7.5' quadrangle) of the field area is within the Bitterroot metamorphic core complex (BMCC) and includes Lolo Peak. Previous mapping in the area was conducted by Nold (1968) and Lewis (1998).

Geologic Setting

The Idaho batholith is a 39,000 km² plutonic complex in the northern Rocky Mountains of central Idaho and western Montana (King and Valley, 2001). The main phases of the batholith are mesozonal (5-15 km) and Late Cretaceous in age (King and Valley, 2001). Lesser, epizonal (< 10 km) Tertiary plutons intrude the Cretaceous main phase granites as well as the surrounding Paleozoic metasedimentary country rocks (King and Valley, 2001). The formation of the batholith is attributed to a mixing of magmas and crustally derived melts produced by subduction along the western margin of North America ~50 to ~100 Ma (Mueller and others, 1995).

The main part of the batholith (Figure 2) is divided into two sections, the northern Bitterroot lobe (14,000 km²) and the southern Atlanta lobe (25,000 km²), that are separated by regionally metamorphosed Precambrian Belt Supergroup sedimentary rocks of the Salmon River arch (King and Valley, 2001).

The Bitterroot lobe of the Idaho batholith was emplaced within high-grade (including sillimanite zone) rocks of the Belt Supergroup about 50 to 90 Ma (Hyndman, 1984). The lobe contains two main Cretaceous phases: hornblende-biotite tonalite/quartz diorite plutons and muscovite-biotite-granodiorite/monzogranite plutons (King and Valley, 2001). Tertiary epizonal plutons intrude the IBB, and have been described as anorogenic plutons (A-type) that formed as a result of continental extension (King and Valley, 2001). These anorogenic plutons are described as a bimodal suite, consisting of predominantly pink granite and gray quartz monzodiorite (King and Valley, 2001). The BMCC comprises the northeastern border zone of the IBB; the formation and exhumation of the complex is coupled with deformational features apparent in the central part of the IBB (Hyndman, 1980).

Previous studies (Nold, 1968, 1974; Hyndman and others, 1988; Lewis et al., 1998; House and others, 2002) have shown that although the Skookum Butte stock is generally interpreted as a granodiorite stock, the pluton exhibits a range of compositions. The southern and southeastern zones are composed of foliated quartz diorite that intrudes upper amphibolite facies metaquartzites, calc-silicate gneisses, and pelitic schists, whereas the northern and western margins consist of a massive, biotite granite that intrudes biotite zone metaquartzites and calc-silicate gneisses.

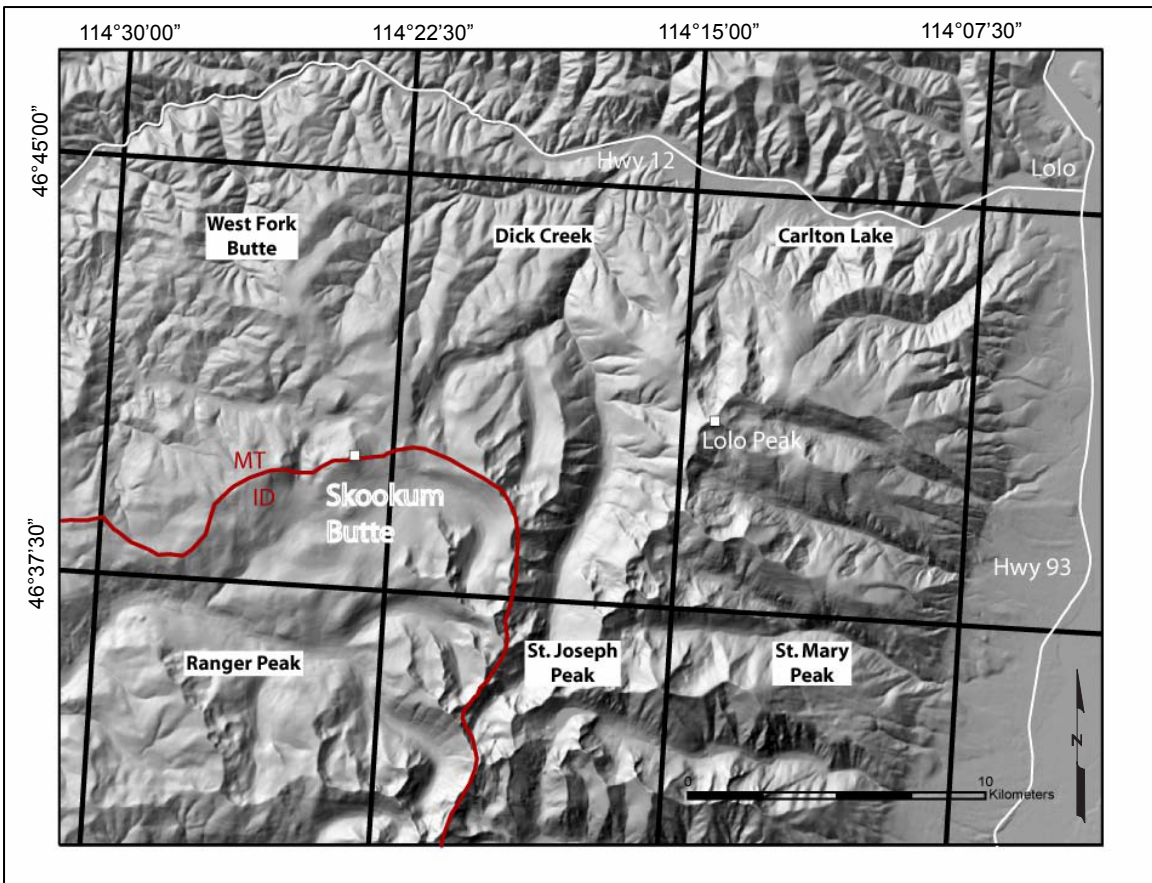


Figure 1. Generalized location map of field area.

The BMCC extends north-south for ~100 km (Chase and Talbot, 1973) and is defined to the east by a gently dipping mylonitic detachment zone. This zone averages about 0.5 km thick (Hyndman, 1980). The dominant metamorphic rock types that comprise the northeastern part of the complex, exposed along Carlton Ridge and Lolo Peak, are quartzofeldspathic gneisses and pelitic schists, which correlate to the Ravalli and Prichard formations of the Proterozoic Belt Supergroup (Nold, 1968).

Methods

The Skookum Butte stock was mapped in order to establish the petrological and structural complexity of the stock. Contacts in this area were assumed to be gradational (Nold, 1968) and were examined in detail in order to provide information on the mechanisms of emplacement. Thin sections were made from samples representative of each lithology; mineral assemblages and rock type were confirmed through petrographic analysis (Table 1). Differentiation between units was determined largely from mapping lithologic variations and fabric development in the field and discriminating magma compositions and sources through whole-rock geochemical analysis (Table 2).

The northeast part of the BMCC was mapped to determine the distribution of metamorphic rocks types, range of metamorphic grade, and correlation between mineral assemblages with the margin of the batholith. Samples of pelitic schists, gneisses, migmatites, and garnet amphibolites were collected.

Map Descriptions

- Qgt** **Glacial deposits** (Holocene and Pleistocene) Unconsolidated till, outwash and other glacial drift including poorly sorted deposits of boulders and finer material.
- Tkg** **Granitic rocks** (Eocene and Cretaceous)
Primarily medium-grained, nonfoliated biotite granite but also includes both foliated and non-foliated fine-grained biotite granodiorite, biotite-hornblende granodiorite, hornblende monzogabbro, and quartz monzodiorite. Equigranular rocks at Skookum Butte are similar both in appearance and geochemistry to Eocene and Cretaceous granitoids of the IBB (Lewis and others, 1992).
- TKgd** **Biotite granodiorite** (Tertiary and Cretaceous)
Granitic lithologies in the northeast border zone of the Idaho-Bitterroot batholith are comprised of a mix of granodiorite and granitic plutons emplaced during the Late Cretaceous from ~75 to 48 Ma. They rose to a depth of ~15-25 km during their emplacement (House et al., 2002). These rocks are fine- to medium-grained. Some outcrops exhibit weak foliation; in others it is absent
- Kmg** **Monzogabbro and monzodiorite** (Cretaceous?)
Foliated, medium-grained, biotite- and hornblende-biotite monzogabbro and monzodiorite.
- Ywcs** **Calc-silicate member of the Belt Supergroup** (Middle Proterozoic)
The lithologies that comprise this unit formed from the metamorphism of the middle member of the Wallace Group. The rocks are layered with green diopside, quartz, feldspathoids, and black hornblende. The layers within the beds comprise the calc-silicate gneiss seen most commonly in outcrop (Nold, 1968).
- Yq** **Quartzite of the Belt Supergroup** (Middle Proterozoic)
Metamorphic quartzite with minor amounts of schist and phyllite. Wehrenberg (1971) and Winston and Link (1993) located this member to be at structurally lower levels than the Wallace Group and therefore placed the Yq in the Ravalli Group. Wallace and others (1990) correlated these rocks with the Mount Sheilds formation. Based on their relative position, it is more likely that they are the metamorphosed equivalents of the Ravalli Group.
- Yqfg** **Quartzofeldspathic gneiss of the Belt Supergroup** (Middle Proterozoic)
Contains areas of unmapped granitic sills and dikes. Quartz content averages 51% and biotite 13% in the southwest part of the area (Chase, 1973), where based on the rock indicates a sedimentary origin. The lithology is predominantly gray-weathering, quartzofeldspathic gneiss with minor amounts of sillimanite and muscovite (Anderson, 1959; Wehrenberg, 1971; Chase, 1977). Chase (1977) correlated these rocks with the Ravalli Group of the Belt Supergroup, but previous assignments to the Prichard Formation (Anderson, 1959; Wehrenberg,

1971; Chase, 1973) are more likely due to the general lack of quartzite within the unit.

Ysgn Schist and gneiss of the Belt Supergroup (Middle Proterozoic)

Lithologies along Carlton Range are characterized by two units: a pelitic schist and quartzofeldspathic gneiss. The units have been described as a brown-weathering biotite and muscovite-biotite schist, biotite-sillimanite gneiss, muscovite-biotite quartzite, and minor calc-silicate rocks (Langton, 1935). Quartz content averages 38%, biotite 24%, and sillimanite 12% in the southern part of the area (Anderson, 1959; Chase, 1973). Typically has feldspar augen, and contains abundant unmapped granitic sills and dikes, as well as minor amounts of garnet amphibolite (metamorphosed mafic sills). Previous workers have correlated these rocks to the oldest rocks in the area thereby connecting them with the Prichard Formation.

Ysgnm Migmatites of the Belt Supergroup (Middle Proterozoic)

Gray to brown weathering migmatites are located around Carlton Lake and the adjacent ridge to the south. These rocks outcrop in the greatest abundance in the brown weathering schists and gneisses of the Ysgn. The migmatites contain abundant lenses and pods of amphibolite that have interpreted to have been emplaced in the Prichard prior to, or during metamorphism (Schafer, 1998).

Age and Lateral Relationship of Map Units

Period/Eon	Epoch/Era	Map Units						
Quaternary	Holocene	Qgt						
	Pleistocene							
Tertiary	Pliocene							
	Miocene							
	Oligocene							
	Eocene							
	Paleocene							
	Late	Kmg						
Cretaceous	Early	TKgd						
	Late							
Proterozoic	Middle	<table border="1"> <tr> <td>Ywcs</td> <td>Yq</td> </tr> <tr> <td>Yqfg</td> <td></td> </tr> <tr> <td>Ysgn</td> <td>Ysgnm</td> </tr> </table>	Ywcs	Yq	Yqfg		Ysgn	Ysgnm
Ywcs	Yq							
Yqfg								
Ysgn	Ysgnm							
Early								

Map Symbols

— Contact

— — — Fault, dashed where inferred

===== + + + Dike, dashed where inferred



Strike and dip of bedding



Strike and dip of foliation

References

- Anderson, R.E., 1959, Geology of lower Bass Creek Canyon, Bitterroot Range, Montana: Missoula, University of Montana, M.S. thesis, 70 p., scale 1:20,000.
- Chase, R.B., and Talbot, J.L., 1973, Structural evolution of the northeastern border zone of the Idaho batholith western Montana: Geological Society of America, v. 5, no. 6, p. 470-471.
- Chase, R.B., 1977, Structural evolution of the Bitterroot dome and zone of cataclasis *in* Chase, R.B. and Hyndman, D.W., eds., Mylonite detachment zone, eastern flank of Idaho batholith: Geological Society of America, Rocky Mountain Section, 30th Annual Meeting, Field Guide 1, p. 1-24, scale 1:200,000 (approximate).
- House, M., Bowring, S., and Hodges, K., 2002, Implications of middle Eocene epizonal plutonism for the unroofing history of the Bitterroot metamorphic core complex, Idaho-Montana: Geological Society of America Bulletin, v. 114, p. 448-461.
- Hyndman, D.W., 1980, Bitterroot dome-Sapphire tectonic block, an example of a plutonic-core gneiss-dome complex with its detached suprastructure: Geological Society of America, v. 153, p. 427-443.
- Hyndman, D.W., 1984, A petrographic and chemical section through the northern Idaho batholith: Journal of Geology, v. 92, p. 83-102.
- Hyndman, D.W., Alt, D., and Sears, J.W., 1988, Post-Archean metamorphism and tectonic evolution of western Montana and northern Idaho, *in* Ernst, W.G., ed., Metamorphism and crustal evolution of the western United States: Englewood Cliffs, New Jersey, Prentice-Hall, p. 332-361.
- King, E., and Valley, J., 2001, The source, magmatic contamination, and alteration of the Idaho batholith, *Contributions to Mineralogy and Petrology* **142** (2001), pp. 72–88.
- Langton, C.M., 1935, Geology of the northeastern part of the Idaho batholith and adjacent region in Montana: Journal of Geology, v.43, no.1, p. 27-60.
- Lewis, R.S., and Frost, T.P., 1992, Geology and petrology of the northern part of the Bitterroot Lobe, Idaho batholith; a preliminary report: Geological Society of America, v. 24, no. 5, p.64.
- Lewis, R.S., 1998, Geologic map of the Montana part of the Missoula West 30' x 60' quadrangle: Montana Bureau of Mines and Geology, Open File Report 373, 20 p., 2 sheet, scale 1:100,000.
- Mueller, P.A., Shuster, R.D., D'Arcy, K.A., Heatherington, A.L., Nutman, A.P., and Williams, I.S., 1995, Source of the Northeastern Idaho Batholith: Isotopic

Evidence for a Paleoproterozoic Terrane in the Northwestern U.S.: The Journal of Geology, v. 103, no. 1, p. 63-72.

Nold, J.L., 1968, Geology of the northeastern border zone of the Idaho Batholith, Montana and Idaho. Ph.D. Thesis, U. of Montana, Missoula. p.159.

Nold, J.L., 1974, Geology of the northeastern border zone of the Idaho batholith, Montana and Idaho: Northwest Geology, v. 3, p. 47-52.

Schafer, C. M., 1998, High grade metamorphism, melting, and migmatization in the Bitterroot Range, Montana-Idaho: Missoula, University of Montana M.S. thesis, p. 81

Wallace, C.A., Lidke, D.J., and Schmidt, R.G., 1990, Faults in the Lewis and Clark Line and fragmentation of the Late Cretaceous foreland basin in the west-central Montana: Geological Society of America Bulletin, v. 102, p. 1021-1037.

Wehrenberg, J.P., 1971, The infrared absorption spectra of scapolite: The American Mineralogist, v. 56, p. 1639.

Winston, D., and Link, P.K., 1993, Middle Proterozoic rocks of Montana, Idaho and eastern Washington: The Belt Supergroup, *in* Reed, Jr., J.C., Bickford, M.E., Houston, R.S., Link, P.K., Rankin, D.W., Sims, P.K., and Van Schmus, W.R., eds., Precambrian; conterminous U.S.: Boulder, Colorado, Geological Society of America, The geology of North America, v. C-2, p. 487-517.

Table 1. Mineral assemblages and rock types.

Sample	Easting	Northing	Rock Type	Lithology	Qtz	Plag	Ksp	Bt	Msc	Hbl	Chl	Sph	Cpx	Deformational Fabric	Petrographic description
SB3	697335	5172232	TKg	Bt Grandiorite	x	x	x	x	x	x	x	x	x	no fabric	medium-grained, hypidiomorphic, some bt altered to chl, high % of microcrystalline qtz w/sutured boundaries
SB22	70227	5170956	TKg	Bt-Hbl Granite	x	x	x	x	x	x	x	x	x	no fabric	coarse-grained, hypidiomorphic, mymekitic, hbl phenocrysts, some bt altering to chl
SB58	703912	5171027	TKg	Bt-Hbl Granite	x	x	x	x	x	x	x	x	x	no fabric	coarse-grained, hypidiomorphic, some bt altering to chl, abundant large sph phenocrysts
SB60	700988	5171231	TKg	Bt-Hbl Granite	x	x	x	x	x	x	x	x	x	no fabric	coarse-grained, hypidiomorphic, some bt altering to chl
SB84	701949	5173025	TKg	Bt-Hbl Granite	x	x	x	x	x	x	x	x	x	no fabric	coarse-grained, hypidiomorphic, some bt altering to chl
SB87	701306	5172602	TKg	Bt-Hbl Granite	x	x	x	x	x	x	x	x	x	no fabric	coarse-grained, hypidiomorphic,
SB88	701153	5172291	TKg	Bt-Hbl Granite	x	x	x	x	x	x	x	x	x	no fabric	coarse-grained, hypidiomorphic, micigraphic, hbl phenocrysts, high % opaques
SB83	702940	5167746	TKg	Bt-Hbl Granite	x	x	x	x	x	x	x	x	x	no fabric	medium-grained, hypidiomorphic, mymekitic, hbl phenocrysts
SB2	697335	5172232	TKg	Bt-Hbl Grandiorite	x	x	x	x	x	x	x	x	x	no fabric	coarse-grained, hypidiomorphic, porphyritic plagi, hbl phenocrysts, some bt altered to chl, mymekitic texture
SB82	701230	5171925	TKg	Bt-Hbl Qtz Monzodiorite	x	x	x	x	x	x	x	x	x	no fabric	coarse-grained, porphyritic
SB81	701230	5171925	TKg	Bt-Msc Granite	x	x	x	x	x	x	x	x	x	no fabric	coarse-grained, hypidiomorphic, sph phenocrysts
SB1	697640	5171073	TKg	Bt-Msc Granite	x	x	x	x	x	x	x	x	x	no fabric	coarse-grained, hypidiomorphic, small % of msc (mostly at feldspar grain boundaries), mymekitic texture, sutured qtz. boundaries
SB31	699187	5171173	TKg	Bt-Msc Granite	x	x	x	x	x	x	x	x	x	no fabric	coarse-grained, hypidiomorphic, porphyritic plagi, bt altered to chl, very small % of msc, mymekitic texture
SB32	699201	5171133	TKg	Bt-Msc Granite	x	x	x	x	x	x	x	x	x	no fabric	coarse-grained, hypidiomorphic, small % of msc at grain boundaries, qtz w/sutured boundaries
SB91	702940	5167746	TKg	Bt-Msc Granite	x	x	x	x	x	x	x	x	x	no fabric	coarse-grained, hypidiomorphic, bt altered to chl, very small % of msc, feldspar altered to white mica, abundant zircon
SB35	698684	5171427	TKg/mafic enclave	Bt-Msc Granite	x	x	x	x	x	x	x	x	x	deformational foliation	fine to medium-grained, porphyritic
SB42	696346	5173719	TKg	Bt-Msc Grandiorite	x	x	x	x	x	x	x	x	x	no fabric	medium-grained, hypidiomorphic, very small % of msc
SB86a	701306	5172602	TKg	Msc-Bt Granite	x	x	x	x	x	x	x	x	x	deformational foliation	coarse-grained, hypidiomorphic
SB80	703289	5167860	TKg/pegmatite	Msc-Bt Grandiorite	x	x	x	x	x	x	x	x	x	no fabric	pegmatic, hypidiomorphic, high % of msc, small % of bt, white mica formation
SB78	705237	5169684	TKg/mafic enclave	Hbl-Bt Qtz Monzodiorite	x	x	x	x	x	x	x	x	x	deformational foliation	fine to medium-grained, porphyritic, hbl phenocrysts
SB47	702735	5170946	Kmg	Hbl-Bt Qtz Monzodiorite	x	x	x	x	x	x	x	x	x	no fabric	medium-grained, porphyritic, mymekitic, hbl phenocrysts, bt altered to chl
SB10	700042	5171079	Kmg	Hbl-Bt Monzogabbro	x	x	x	x	x	x	x	x	x	no fabric	medium-grained, porphyritic, hbl phenocrysts
SB43	696409	5173315	Kmg	Hbl-Bt Monzogabbro	x	x	x	x	x	x	x	x	x	no fabric	medium-grained, porphyritic, hbl phenocrysts
SB45	702938	5170929	Kmg	Hbl-Bt Monzogabbro	x	x	x	x	x	x	x	x	x	no fabric	medium-grained, porphyritic, hbl phenocrysts
SB86b	701306	5172602	Ysgn/pegmatite	Bt-Msc Gneiss	x	x	x	x	x	x	x	x	x	deformational foliation	medium-grained to pegmatitic, hypidioblastic, hypidiomorphic
SB83	704405	51707314	Ysgn/leucosome	Bt-Msc Gneiss	x	x	x	x	x	x	x	x	x	deformational foliation	medium-grained, hypidioblastic, hypidiomorphic
SB84	703047	5168262	Ysgn/leucosome	Bt-Msc Gneiss	x	x	x	x	x	x	x	x	x	deformational foliation	medium-grained, hypidioblastic, hypidiomorphic
SB70	702335	5173305	Ysgn/leucosome	Hbl-Bt Gneiss	x	x	x	x	x	x	x	x	x	deformational foliation	medium-grained, hypidioblastic, hypidiomorphic
SB82	702940	5167746	Ysgn	Hbl-Bt Gneiss	x	x	x	x	x	x	x	x	x	deformational foliation	fine to medium-grained, hornfels
SB89	703289	5167860	Ysgn/leucosome	Msc-Bt Gneiss	x	x	x	x	x	x	x	x	x	deformational foliation	medium-grained, hypidioblastic, hypidiomorphic
SB7	696297	5172884	Ywcs	Diopsidic Calc-silicate	x	x	x	x	x	x	x	x	x	no fabric	coarse-grained, hypidioblastic, porphyritic texture
SB20	702406	5170968	Ywcs	Diopsidic Calc-silicate	x	x	x	x	x	x	x	x	x	no fabric	coarse-grained, hypidioblastic

Note: UTM Zone 11.

Explanation:

Bt = biotite

Chl = chlorite

Cpx = clinopyroxene

Hbl = hornblende

Msc = muscovite

Ksp = potassium feldspar

Plag = plagioclase

Sph = sphene

Table 2. Whole rock geochemical analyses

Oxide/Element		SB1	SB2	SB3	SB7	SB10	SB20	SB22	SB31	SB32	SB35	SB42
SiO ₂	%	73.15	64.6	69.88	56.52	49.67	58.76	71.76	71.99	72.81	74.11	73.82
Al ₂ O ₃	%	14.11	17.35	16.1	8.21	17.06	9.14	14.3	14.28	14.35	13.3	13.34
Fe ₂ O ₃ (T)	%	1.42	2.94	2.12	4.99	10.29	5.2	1.78	1.87	1.64	2.16	2.38
MnO	%	0.029	0.026	0.02	0.122	0.133	0.16	0.027	0.036	0.023	0.007	0.014
MgO	%	0.37	1.64	1.14	8.87	6.4	10.69	0.5	0.43	0.41	0.76	1.43
CaO	%	1.3	3.73	3.7	16.04	9	10.65	1.59	1.54	1.47	1.77	2.57
Na ₂ O	%	3.5	4.34	4.54	2.86	3.29	2.83	2.9	3.52	3.5	4.44	3.55
K ₂ O	%	4.57	2.86	1.2	0.24	1.13	1.88	5.81	4.46	4.39	1.21	1.41
TiO ₂	%	0.169	0.358	0.267	0.484	1.318	0.429	0.194	0.207	0.231	0.321	0.355
P ₂ O ₅	%	0.08	0.34	0.02	0.17	0.28	0.06	0.09	0.08	0.08	0.08	0.04
LOI	%	0.61	0.43	0.37 < 0.01		0.98	0.91	0.43	0.59	0.78	0.72	0.74
Total	%	99.29	98.6	99.35	98.51	99.57	100.7	99.38	99.02	99.68	98.88	99.65
Sc	ppm	2	4	3	10	21	19	1	3	3	5	4
Be	ppm	3	1	1	2	1	6	2	3	3	1	1
V	ppm	10	42	31	66	175	67	15	13	16	31	39
Ba	ppm	987	2522	401	79	694	77	2425	1283	1044	251	382
Sr	ppm	250	664	581	296	749	68	435	313	279	214	391
Y	ppm	10	8 < 2		31	15	33	5	12	13	13	7
Zr	ppm	116	154	119	58	129	129	101	159	162	211	165
Cr	ppm	< 20	40	20	40	80	40	< 20	20	< 20	40	30
Co	ppm	2	6	4	11	35	11	3	2	2	3	4
Ni	ppm	< 20	< 20	< 20	30	110	< 20	< 20	< 20	< 20	< 20	< 20
Cu	ppm	10	20 < 10		10	50 < 10		10 < 10	< 10	< 10	10	10
Zn	ppm	40	40 < 30		50	90	120 < 30		40	50 < 30		30
Ga	ppm	18	18	15	10	19	17	15	18	20	14	15
Ge	ppm	1 < 1	< 1		3	1	4 < 1		1	1	1 < 1	
As	ppm	< 5	< 5	< 5	< 5	< 5	< 5	< 5	< 5	< 5	< 5	< 5
Rb	ppm	187	76	45	4	32	152	143	172	171	38	60
Nb	ppm	20	4	3	10	11	12	4	12	13	6	3
Mo	ppm	< 2	< 2	< 2	< 2	< 2	< 2	< 2	< 2	< 2	< 2	< 2
Ag	ppm	< 0.5	< 0.5	< 0.5	< 0.5	< 0.5	< 0.5	< 0.5	< 0.5	< 0.5	< 0.5	< 0.5
In	ppm	< 0.2	< 0.2	< 0.2	< 0.2	< 0.2	< 0.2	< 0.2	< 0.2	< 0.2	< 0.2	< 0.2
Sn	ppm	3	3	1	3	2	3	1	2	2	2	1
Sb	ppm	1.1 < 0.5	< 0.5	< 0.5	< 0.5	< 0.5		5.7 < 0.5	< 0.5	< 0.5	< 0.5	< 0.5
Cs	ppm	5.1	4.2	3.5	< 0.5	0.8	9.6	2.2	3.8	3.3	1.1	2.9
La	ppm	34.4	20.6	2.7	16.6	28.8	11.3	41.9	39.7	34.5	18.2	76.8
Ce	ppm	64	37.5	4.1	55.4	54.9	30	69.9	69.9	62.2	34.1	143
Pr	ppm	6.32	4.03	0.38	8.32	6.45	4.13	6.64	7.47	6.6	3.75	15.9
Nd	ppm	20.6	14.7	1.3	35.5	25.1	17.4	20.7	26.3	22	13.7	57.6
Sm	ppm	3.3	2.7	0.2	7.5	4.6	4	2.5	4.5	3.6	2.4	8.5
Eu	ppm	0.71	0.96	0.78	1.33	1.61	0.66	0.76	0.86	0.77	0.86	1.5
Gd	ppm	2.4	2.4	0.1	6.5	4.2	4.5	1.7	3.3	2.8	2.3	5.8
Tb	ppm	0.4	0.4 < 0.1		1	0.6	0.9	0.2	0.4	0.4	0.4	0.5
Dy	ppm	1.9	1.9	0.1	6	3.3	6	1.1	2.2	2.4	2.4	2.2
Ho	ppm	0.4	0.4 < 0.1		1.1	0.6	1.2	0.2	0.4	0.4	0.5	0.3
Er	ppm	1.1	1	0.1	3.4	1.7	3.7	0.6	1.4	1.3	1.6	0.7
Tm	ppm	0.18	0.14 < 0.05		0.53	0.24	0.57	0.1	0.21	0.21	0.25	0.09
Yb	ppm	1.2	0.9	0.2	3.5	1.5	3.8	0.6	1.4	1.4	1.8	0.6
Lu	ppm	0.18	0.14	0.04	0.54	0.22	0.6	0.09	0.22	0.22	0.28	0.1
Hf	ppm	3.3	4.1	2.9	2.1	3	3.8	2.6	4.2	4.7	5.3	4
Ta	ppm	1.5	0.2	0.2	1.4	0.8	1.3	0.4	1.4	1.4	0.6	0.2
W	ppm	< 1	5	4 < 1	< 1	< 1		1 < 1	< 1	< 1	< 1	1
Tl	ppm	1.3	0.4	0.2 < 0.1		0.2	0.8	0.8	1.1	1.2 < 0.1		0.3
Pb	ppm	42	17	11	6	7	7	33	41	42	7	11
Bi	ppm	< 0.4	< 0.4	< 0.4	0.5 < 0.4		0.5 < 0.4	< 0.4	< 0.4	< 0.4	< 0.4	< 0.4
Th	ppm	19.4	4	0.1	2.4	3.8	4.8	12.7	32.9	21.4	7	27.7
U	ppm	4.4	0.8	0.5	1.7	1	2.5	11.6	6.6	5.5	1.2	1.4

Table 2. Whole rock geochemical analyses

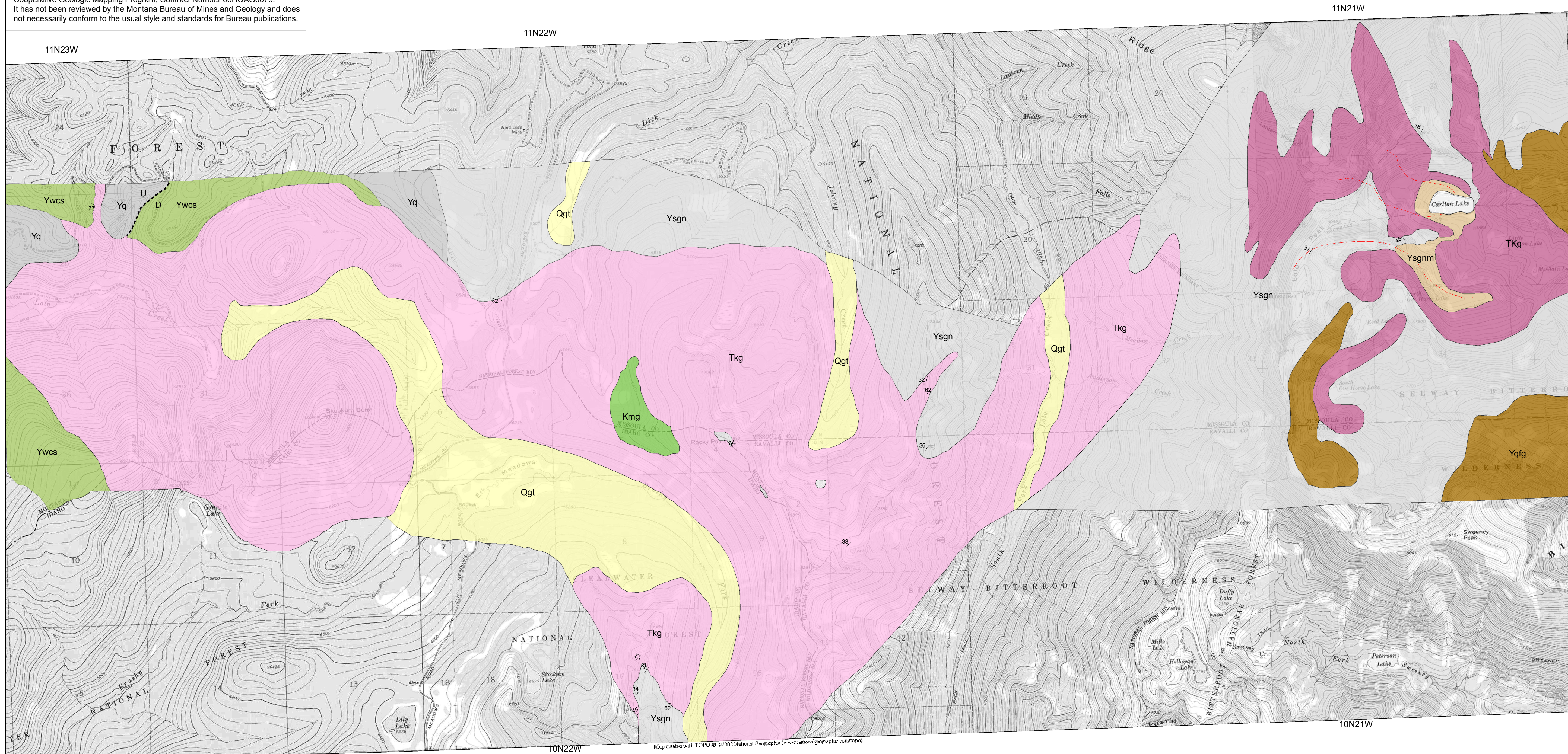
Oxide/Element		SB43	SB45	SB47	SB58	SB60	SB63	SB70	SB78	SB81	SB82	SB84
SiO ₂	%	52.9	54.75	59.25	67.04	71.47	76.15	52.43	62.5	68.12	63.66	64.75
Al ₂ O ₃	%	12.14	16.76	15.81	15.45	14.26	12.48	15.6	15.45	14.87	16.84	16.31
Fe ₂ O ₃ (T)	%	8.68	8.37	6.77	3.86	2.17	3.05	9.22	5.9	2.79	3.79	4.32
MnO	%	0.12	0.121	0.101	0.041	0.029	0.039	0.154	0.083	0.031	0.043	0.054
MgO	%	10.23	3.81	2.81	1.15	0.38	0.76	7.37	1.88	0.83	1.88	1.38
CaO	%	9.13	6.21	4.95	2.83	1.43	1.68	6.44	3.76	2.2	3.52	3.02
Na ₂ O	%	1.97	3.96	3.49	3.57	3.48	2.89	2.32	4.2	3.42	3.94	3.88
K ₂ O	%	1.18	2.1	3.22	4.08	4.85	1.91	2.65	2.76	4.82	3.49	3.94
TiO ₂	%	0.557	1.548	0.891	0.593	0.209	0.453	1.081	1.156	0.406	0.452	0.627
P ₂ O ₅	%	0.11	0.38	0.23	0.23	0.08	0.14	0.21	0.33	0.15	0.23	0.24
LOI	%	2.14	0.85	0.96	0.49	0.41	0.68	1.66	0.61	0.38	0.68	0.72
Total	%	99.16	98.85	98.48	99.34	98.77	100.2	99.14	98.63	98.02	98.52	99.24
Sc	ppm	27	14	16	3	2	7	20	9	5	3	6
Be	ppm	2	2	2	1	2	2	3	2	1	5	2
V	ppm	201	140	104	52	14	35	130	82	36	63	55
Ba	ppm	225	1116	2516	2258	1473	277	561	1872	1832	1782	2139
Sr	ppm	208	704	659	683	359	237	376	711	502	687	587
Y	ppm	35	24	22	11	11	109	18	18	9	8	13
Zr	ppm	89	210	394	236	145	373	150	249	202	121	304
Cr	ppm	570	30	20	30	< 20	50	200	< 20	< 20	50	< 20
Co	ppm	24	25	20	8	5	5	32	13	5	9	9
Ni	ppm	110	30	20	< 20	< 20	< 20	110	30	< 20	< 20	< 20
Cu	ppm	< 10	20	20	20	< 10	10	20	20	< 10	10	20
Zn	ppm	70	110	90	50	< 30	60	140	80	40	60	90
Ga	ppm	18	23	23	19	18	15	20	20	19	20	23
Ge	ppm	2	1	1	< 1	1	2	2	< 1	< 1	1	1
As	ppm	< 5	< 5	< 5	< 5	< 5	< 5	< 5	< 5	< 5	< 5	< 5
Rb	ppm	39	64	69	93	159	81	127	52	118	121	113
Nb	ppm	6	20	13	10	11	8	6	19	8	7	11
Mo	ppm	< 2	< 2	< 2	< 2	< 2	< 2	< 2	< 2	< 2	< 2	< 2
Ag	ppm	< 0.5	< 0.5	< 0.5	< 0.5	< 0.5	< 0.5	< 0.5	< 0.5	< 0.5	< 0.5	< 0.5
In	ppm	< 0.2	< 0.2	< 0.2	< 0.2	< 0.2	< 0.2	< 0.2	< 0.2	< 0.2	< 0.2	< 0.2
Sn	ppm	10	2	2	1	2	2	4	2	1	2	1
Sb	ppm	< 0.5	< 0.5	< 0.5	< 0.5	< 0.5	< 0.5	< 0.5	< 0.5	< 0.5	< 0.5	< 0.5
Cs	ppm	2.1	1.2	0.8	1.6	2.4	3.5	7.8	1	1.9	6.3	1.8
La	ppm	15.8	48.1	168	77	49.9	59.2	17	66.7	67	37.6	88.1
Ce	ppm	46	105	255	132	84.8	129	35.6	117	115	69.5	149
Pr	ppm	6.93	13	24.1	13.2	8.65	14.8	4.12	12.5	11.4	7.36	14.8
Nd	ppm	29.9	49	76.8	42.3	28.5	55.8	17	43.3	36.7	24.7	47.1
Sm	ppm	6.7	8.3	10.5	5.4	4.3	12.4	3.9	6.9	4.6	3.5	6.4
Eu	ppm	2.12	2.14	2.12	1.6	0.85	1.96	1.46	2.22	1.25	0.91	1.59
Gd	ppm	6.4	6.8	7.4	3.7	3.1	13.8	3.9	5.7	3	2.4	4.3
Tb	ppm	1.1	1	1	0.5	0.4	2.8	0.6	0.8	0.4	0.3	0.6
Dy	ppm	6.6	5.2	5.3	2.4	2.2	18.4	3.9	4	1.8	1.5	2.9
Ho	ppm	1.4	1	0.9	0.4	0.4	3.7	0.8	0.7	0.3	0.3	0.5
Er	ppm	4.1	2.6	2.5	1.2	1.2	11.5	2.3	2.1	1	0.8	1.5
Tm	ppm	0.66	0.37	0.33	0.18	0.17	1.84	0.33	0.3	0.15	0.12	0.21
Yb	ppm	4.5	2.3	1.9	1.1	1.1	11.9	2	1.9	0.9	0.8	1.3
Lu	ppm	0.68	0.32	0.27	0.18	0.17	1.72	0.3	0.28	0.14	0.12	0.19
Hf	ppm	2.5	4.6	8.7	5.2	4	9.6	3.8	5.6	4.5	3.2	7
Ta	ppm	0.7	1	1.1	0.9	1.4	0.7	0.5	1.7	0.7	0.9	0.8
W	ppm	< 1	< 1	< 1	3	5	3	< 1	< 1	< 1	< 1	< 1
Tl	ppm	0.1	0.4	0.4	0.6	1	0.4	1	0.3	0.7	0.7	0.8
Pb	ppm	< 5	12	20	26	44	21	9	20	23	21	26
Bi	ppm	0.5	< 0.4	< 0.4	< 0.4	< 0.4	< 0.4	< 0.4	< 0.4	1	1.1	< 0.4
Th	ppm	2.8	4	31.9	14.7	22.3	21.6	14.1	13.8	18.1	12.3	18.8
U	ppm	1.2	1.1	2.1	2.2	3	7.3	3.9	3	4.1	2.7	3.2

Table 2. Whole rock geochemical analyses

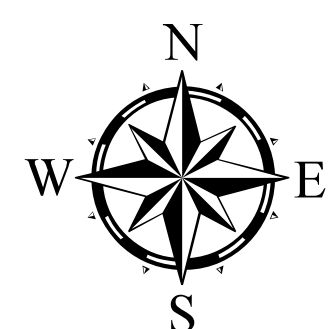
Oxide/Element		SB86	SB87	SB88	SB89	SB90	SB91	SB92	SB93	SB94
SiO ₂	%	82.54	67.22	68.26	71.39	74.66	70.9	54.23	69.16	70.46
Al ₂ O ₃	%	9.84	13.87	15.02	13.22	15.18	14.59	15.71	15.38	13.76
Fe ₂ O ₃ (T)	%	1.5	4.3	3.36	4.91	1	1.73	6.97	3.17	4.64
MnO	%	0.025	0.066	0.045	0.036	0.014	0.029	0.095	0.044	0.034
MgO	%	0.5	3.94	1.02	1.69	0.21	0.6	7.66	0.82	1.69
CaO	%	0.48	3.69	2.45	0.52	2.11	1.82	6.6	2.11	0.77
Na ₂ O	%	2.36	2.49	3.55	1.22	4.45	3.18	2.28	3.58	1.7
K ₂ O	%	2.6	2.28	4.21	3.92	1.72	5.22	2.46	4.58	3.63
TiO ₂	%	0.18	0.472	0.484	0.586	0.072	0.233	1.001	0.407	0.564
P ₂ O ₅	%	0.04	0.13	0.17	0.09	0.09	0.12	0.41	0.18	0.08
LOI	%	0.1	0.87	0.38	1.63	0.57	0.54	1.95	0.39	1.47
Total	%	100.1	99.33	98.93	99.19	100.1	98.96	99.37	99.81	98.79
Sc	ppm	3	10	5	12	2	2	16	4	11
Be	ppm	3	4	2 < 1		4	2	2	3	1
V	ppm	13	68	37	67 < 5		18	124	29	62
Ba	ppm	326	868	1752	1037	383	2191	2260	1774	942
Sr	ppm	63	256	465	144	377	441	1313	480	179
Y	ppm	20	13	13	32	9	6	13	7	29
Zr	ppm	193	184	232	280	26	131	209	252	246
Cr	ppm	< 20	60	30	50 < 20	< 20		380	20	30
Co	ppm	< 1	10	6	4	1	3	32	6	4
Ni	ppm	< 20	20 < 20	< 20	< 20	< 20	< 20	180 < 20	< 20	
Cu	ppm	< 10	< 10	< 10	< 10	10 < 10	< 10	< 10	10	20
Zn	ppm	160	60	60	80 < 30		30	80	70	70
Ga	ppm	12	18	21	20	14	16	21	21	18
Ge	ppm	1	2	1	1	1	1	1	1	1
As	ppm	< 5	< 5	< 5	< 5	< 5	< 5	< 5	< 5	< 5
Rb	ppm	130	159	126	147	50	141	75	140	135
Nb	ppm	7	9	11	10	4	4	8	8	9
Mo	ppm	< 2	< 2	< 2	< 2	< 2	< 2	< 2	< 2	< 2
Ag	ppm	< 0.5	< 0.5	< 0.5	< 0.5	< 0.5	< 0.5	< 0.5	< 0.5	< 0.5
In	ppm	< 0.2	< 0.2	< 0.2	< 0.2	< 0.2	< 0.2	< 0.2	< 0.2	< 0.2
Sn	ppm	6	4	2	4	2	1	1	2	3
Sb	ppm	< 0.5	< 0.5	< 0.5	< 0.5	< 0.5	1.7 < 0.5	< 0.5	< 0.5	< 0.5
Cs	ppm	3.1	11.2	2.3	5	2.1	2.7	3.6	3.3	4.9
La	ppm	18	22.2	81.3	39.1	8.3	49.2	63.6	79.8	34.9
Ce	ppm	38.4	42.4	142	81	16.3	81.3	120	142	70.9
Pr	ppm	4.55	4.75	14.3	9.38	1.88	7.86	13.6	14.7	8.23
Nd	ppm	16.9	17.7	45.8	35.5	7	24.9	49.5	48	31
Sm	ppm	3.7	3.1	6.2	6.8	1.5	3	7.1	6.6	5.9
Eu	ppm	0.58	0.72	1.34	1.39	0.78	0.88	2.2	1.4	1.28
Gd	ppm	3.4	2.8	4.2	6.2	1.4	2	4.8	4	5.3
Tb	ppm	0.6	0.5	0.5	1	0.3	0.2	0.6	0.5	0.9
Dy	ppm	3.4	2.7	2.7	5.7	1.7	1.2	3	2	5.1
Ho	ppm	0.7	0.5	0.5	1.1	0.4	0.2	0.5	0.3	1.1
Er	ppm	1.9	1.7	1.4	3.6	1.1	0.7	1.5	0.8	3.3
Tm	ppm	0.3	0.26	0.2	0.54	0.18	0.1	0.21	0.1	0.51
Yb	ppm	2	1.7	1.2	3.5	1.2	0.7	1.3	0.6	3.3
Lu	ppm	0.3	0.26	0.17	0.54	0.2	0.11	0.19	0.09	0.52
Hf	ppm	5.2	4.9	5.5	7.4	0.8	3.2	5.1	5.8	6.5
Ta	ppm	0.9	1.2	1.1	0.7	0.5	0.4	0.6	0.6	0.6
W	ppm	< 1	1	1 < 1		3 < 1		1	1 < 1	
Tl	ppm	0.8	0.8	0.8	0.8	0.2	0.8	0.5	0.9	0.7
Pb	ppm	36	9	26	22	28	35	11	26	27
Bi	ppm	< 0.4	0.4 < 0.4		0.8 < 0.4	< 0.4	< 0.4	< 0.4	< 0.4	0.4
Th	ppm	6	3.9	22.1	13.6	3	13.4	7.8	25.5	12.1
U	ppm	2.5	1.4	3	3.7	2.4	10.1	1.8	1.3	2.5

Montana Bureau of Mines and Geology
EDMAP 4 - Plate 1 of 2

This report was prepared by geology students under the direction of his advisor as a product of the EDDMAP Component of the U.S. Geological Survey National Cooperative Geologic Mapping Program, Contract Number 06HQAG0079. It has not been reviewed by the Montana Bureau of Mines and Geology and does not necessarily conform to the usual style and standards for Bureau publications.



Geologic Map of Parts of the Carlton Lake, Dick Creek, and West Fork Butte 7.5 quadrangles Northwest Montana
GIS by Connie Brown and Colleen Fitzpatrick
UTM Zone 11 NAD 83 2009



Map Units

Qgt	Yq
TKg	Yqfg
TKgd	Ysgn
Kmg	Ysgnm
Ywcs	

Map Symbols

▲	Foliation
—	Strike and Dip
- - - - -	Dike
-----	Fault

This report was prepared by geology students under the direction of his advisor as a product of the EDMAP Component of the U.S. Geological Survey National Cooperative Geologic Mapping Program, Contract Number 06HQAG0079. It has not been reviewed by the Montana Bureau of Mines and Geology and does not necessarily conform to the usual style and standards for Bureau publications.

Sample Locations

